JGR Atmospheres

RESEARCH ARTICLE
10.1029/2024JD042040

Dual Role of Aerosols on Reactive Bromine Recycling in Extrapolar Marine and Continental Regions

Yingnan Zhang[1], Xiaorui Chen[1,2], Tao Wang[1], Qinyi Li[1,3], Men Xia[4], Mingxue Li[1], Jiangshan Mu[3], Hengqing Shen[1,3], Hartmut Herrmann[5,6], and Likun Xue[3]

[1]Department of Civil and Environmental Engineering, The Hong Kong Polytechnic University, Hong Kong, China, [2]Southern Marine Science and Engineering Guangdong Laboratory (Zhuhai), School of Atmospheric Sciences, Sun Yat-sen University, Zhuhai, China, [3]Environment Research Institute, Shandong University, Qingdao, China, [4]Faculty of Science, Institute for Atmospheric and Earth System Research, University of Helsinki, Helsinki, Finland, [5]School of Environmental Science and Engineering, Shandong University, Qingdao, China, [6]Atmospheric Chemistry Department (ACD), Leibniz Institute for Tropospheric Research (TROPOS), Leipzig, Germany

Abstract Reactive bromine species play important roles in atmospheric chemistry and influence the abundance of climate- and air quality-relevant trace gases. While extensive studies have focused on bromine chemistry in polar regions, the bromine species in extrapolar regions, particularly regarding pollution-related bromine recycling, have received less attention. In this study, we examine the factors influencing the bromine recycling at a clean marine site of the North Atlantic (Cape Verde, CVAO), a semipolluted coastal site of the South China Sea (Hok Tsui, HT), and a polluted continental site of North China (Wangdu, WD), using an observation-based model combined with updated halogen chemistry. Our results indicate that aerosol-related multiphase processes significantly affect bromine recycling in these extrapolar sites. Nitrate photodissociation efficiently recycled bromide into the gas phase in regions characterized by strong aerosol acidity (HT) or high aerosol concentrations (WD). Concurrently, bromine species are lost from the gas phase toward aerosol surfaces, with this process being more effective at higher liquid water content (WD > HT > CVAO). In semipolluted and polluted sites, the aerosol-related processes resulted in elevated bromine levels in the daytime compared to nighttime, leading to larger effects of bromine species on ozone than previously thought. Our study suggests the need for a better understanding of the complex effects of aerosols on reactive halogen chemistry.

Plain Language Summary Reactive bromine species significantly influence the abundance of climate- and air quality-relevant trace gases. Over the past decades, the sources and atmospheric impacts of bromine species in polar regions have been extensively studied due to their critical role in the Arctic ozone depletion episodes (ODEs). Both observations and laboratory studies have identified aerosols as crucial players in bromine explosions and subsequent Arctic ODEs. Here, using an observation-constrained multiphase chemical box model with updates in halogen chemistry, we demonstrate that aerosols can provide a medium for bromine species activation or loss in extrapolar marine and continental regions, depending on their compositions and properties. These aerosol-related processes are not included in current chemistry climate models, potentially hindering the accurate assessment of the impact of halogen species on climate and air quality.

Key Points:

- We updated bromine-aerosol interaction mechanisms and improved bromine simulations across extrapolar marine and continental regions
- Aerosols can provide a medium for bromine species activation or loss, depending on aerosol compositions and properties
- Overlooking aerosol-related processes may underestimate the effects of bromine species on ozone in semi-polluted and polluted regions

Yingnan Zhang and Xiaorui Chen contributed equally to this work.

Supporting Information:

Supporting Information may be found in the online version of this article.

Correspondence to:

T. Wang and Q. Li,
tao.wang@polyu.edu.hk;
qinyi.li@sdu.edu.cn

Citation:

Zhang, Y., Chen, X., Wang, T., Li, Q., Xia, M., Li, M., et al. (2024). Dual role of aerosols on reactive bromine recycling in extrapolar marine and continental regions. *Journal of Geophysical Research: Atmospheres*, *129*, e2024JD042040. https://doi.org/10.1029/2024JD042040

Received 24 JUL 2024
Accepted 18 NOV 2024

1. Introduction

Reactive bromine species ($Br_y = 2 \times Br_2 + BrNO_2 + BrCl + Br + BrO + BrNO_3 + HOBr$) are important players of atmospheric chemistry and influence the abundance of climate- and air quality-relevant trace gases (Li et al., 2022; Saiz-Lopez et al., 2023). Since discovering their links to ozone depletion episodes (ODEs) in the Arctic during the 1980s (Barrie et al., 1988; Bottenheim et al., 1986; Oltmans & Komhyr, 1986), the sources and atmospheric impacts of bromine species in polar regions have been extensively studied (Abbatt et al., 2012; Platt & Hönninger, 2003; Saiz-Lopez & von Glasow, 2012; Simpson et al., 2007, 2015). The occurrence of Arctic ODEs is commonly associated with strong winds, which carry large amounts of blowing snow particles aloft. These particles facilitate autocatalytic chemical chain reactions, leading to the release of reactive bromine species (known as bromine explosion) and subsequent ozone depletion (McElroy et al., 1999; Wennberg, 1999). These findings underscore the important role of aerosols in bromine activation since the production of reactive bromine

species (e.g., Br_2 and BrCl, the key precursors of Br radical) commonly involves multiphase and aerosol bulk reactions (Hoffmann et al., 2019; Saiz-Lopez & von Glasow, 2012; Simpson et al., 2015).

Over the past decades, interest in reactive bromine chemistry has expanded to extrapolar regions, which have a large burden of aerosols from natural and anthropogenic sources on a global scale. Reactive bromine species were detected over the pristine marine boundary layer (MBL), in tidal coastal areas, and in pollution-laden air mass (Simpson et al., 2015). The reactive bromine species in the extrapolar regions cannot be reproduced by the chemical mechanisms developed from polar studies (Peng et al., 2020; Sommariva & von Glasow, 2012; Xia et al., 2022). In the MBL atmosphere, chemical models incorporating the polar study-based mechanism predict abundant bromine levels (up to 50 pptv, with BrCl being the most abundant species), primarily from sea salt aerosol debromination (Parrella et al., 2012). This contradicts measurements at Cape Verde, a remote marine site in the North Atlantic, where only low levels of BrO (2.5 ± 1.1 pptv) and below detection limit (2 pptv) levels of BrCl were measured (Sommariva & von Glasow, 2012). Field measurements at a polluted coastal site in Hong Kong (Xia et al., 2022) and a polluted continental site in northern China (Peng et al., 2020) observed significant daytime levels of Br_2 and BrCl. Neither the abundance nor the diurnal profile can be fully reproduced via the chemical models with the previously known bromine chemistry. Laboratory experiments suggest bromide activation by particulate nitrate (NO_3^-) photodissociation as an important daytime Br_2 source (Xia et al., 2022). There is a need for a better understanding of the aerosol-related processes that affect the bromine sources and sinks in extrapolar regions and their environmental impacts, in view of varying aerosol compositions and properties (e.g., acidity and aerosol water content) between extrapolar regions and polar regions.

Within the present study, we show that aerosols can provide a medium for bromine species activation or loss based on the comprehensive observations at the Hok Tsui coastal site (Xia et al., 2022). Using an observation-constrained multiphase chemical box model integrated with updated halogen chemistry, especially with updates in the interactions between bromine species and aerosols, we investigate the mechanisms of how aerosols affect the gas-to-aqueous bromine partition and the gas-phase bromine speciation in the remote marine, semi-polluted coastal, and polluted continental regions where aerosol compositions and properties largely differed. We also discuss the potential impacts of the aerosol-related multiphase processes on the role of reactive bromine species in the ozone formation and loss. Our findings bridge the gap between bromine simulations and observations in extrapolar regions and provide insight into the complex effects of aerosols on bromine chemistry.

2. Materials and Methods

2.1. Observational Data Sets

Diurnal data on bromine species and supporting data were collected from published literature and our previous measurements (Table S1 in Supporting Information S1). These data sets encompass three extrapolar sites that represent different chemical conditions (Figure S1 in Supporting Information S1). The specific species or parameters measured at each site, along with the corresponding instrument techniques, are provided in Table S1 in Supporting Information S1.

The semipolluted coastal site of Hok Tsui (HT) is located in Hong Kong, Southern China. The measurements include Br_2, BrCl, NO, NO_2, O_3, SO_2, CO, VOCs, HONO, N_2O_5, Cl_2, HOCl, $ClNO_2$, BrCl, Br_2, NH_3, $PM_{2.5}$, NO_3^-, SO_4^{2-}, NH_4^+, Cl^-, organics, aerosol surface and volume concentrations, temperature, pressure, relative humidity, and the photolysis frequency of NO_2 ($J(NO_2)$). The HT site is characterized by moderate aerosol abundance (e.g., aqueous NO_3^- concentrations: 1.75 mol/L), strong aerosol acidity (pH: 2.31), and high aerosol liquid water content (LWC; 6.29 μg/m^3).

The remote maritime site of Cape Verde (CVAO) is located in the tropical North Atlantic upwelling region off the coast of West Africa. We obtained measurements of BrO, NO, NO_2, O_3, CO, VOCs, HONO, NO_3^-, SO_4^{2-}, NH^{4+}, Cl^-, Br^-, Na^+, Ca^{2+}, Mg^{2+}, K^+, aerosol number, surface, volume concentrations, temperature, pressure, relative humidity, and $J(NO_2)$. The CVAO site is marked by moderate aerosol abundance (e.g., aqueous NO_3^- concentrations: 0.98 mol/L), weak aerosol acidity (pH: 4.91), and moderate aerosol LWC (2.31 μg/m^3).

The polluted continental site of Wangdu (WD) is located in northern China. We obtained measurements of HOBr, BrCl, Br_2, NO, NO_2, O_3, SO_2, CO, VOCs, HONO, N_2O_5, Cl_2, HOCl, $ClNO_2$, NH_3, $PM_{2.5}$, NO_3^-, SO_4^{2-}, NH_4^+, Cl^-, Br^-, organics, aerosol surface concentration, temperature, pressure, relative humidity, and $J(NO_2)$. The WD

site is characterized by high aerosol abundance (e.g., aqueous NO_3^- concentrations: 14.28 mol/L), weak aerosol acidity (pH: 4.70), and high aerosol LWC (7.17 μg/m^3).

Five-minute average observations of Br_2, BrCl, and other species and parameters at HT were used to examine potential bromine sources and sinks (refer to Xia et al. (2022) for details on field observations at HT). Additionally, the observational data collected from HT, alongside the data sets from CVAO and WD, were used as input to the chemical box model to examine dominant factors influencing the bromine recycling in these extrapolar areas.

2.2. Development of Halogen Chemistry Module

We developed three chemistry modules to assess the impact of aerosol-related multiphase processes on bromine chemistry. All modules were based on the Master Chemical Mechanism (MCM) v3.3.1 (Jenkin et al., 2003; Saunders et al., 2003) but differed in their treatment of halogen chemistry.

The first module ("MECH_EX") denotes existing polar study-based mechanisms, incorporating gas-phase reactions and heterogeneous uptake of chlorine and bromine species (Ammann et al., 2013; Li et al., 2021; Xia et al., 2022; Refer to Text S1 in Supporting Information S1 for details), and S(IV) oxidation by HOBr (Liu & Abbatt, 2020). In this module, heterogeneous uptake reactions were implemented as first-order gas-phase loss reactions.

The second module ("MECH_NO_3^-") extends "MECH_EX" by incorporating Br_2 production through nitrate photodissociation (Equation 1) (Xia et al., 2022).

$$P(\mathrm{Br_2}) = k \times \left[\mathrm{H^+}\right] \times \left[\mathrm{NO_3^-}\right] \times \left[\mathrm{Br^-}\right] \times J(\mathrm{Br_2}) \times S_a \quad (1)$$

where k denotes an empirical prefactor and was determined as 758; [H^+], [NO_3^-], and [Br^-] represent the aqueous-phase H^+, NO_3^-, and Br^- concentrations in fine aerosols, respectively; $J(Br_2)$ represents a measure of light intensity; and S_a represents the aerosol surface area.

The third module ("MECH_PT") extends "MECH_NO_3^-" by implementing the heterogeneous loss of each bromine species (e.g., Br_2, $BrNO_2$, $BrNO_3$, BrO, BrCl, HOBr, and HBr) on aerosol surfaces (Equations 2 and 3). Here, the heterogeneous loss was implemented by incorporating phase transfer (PT) processes from the Chemical Aqueous-Phase RAdical Mechanism (CAPRAM) (Ervens et al., 2003; Hoffmann et al., 2019), which are summarized as follows: (a) mass transport of the gaseous bromine species to the air-water interface, (b) transfer across the interface (accommodation process), (c) mass transport of the dissolved bromine species within the aqueous phase, (d) aqueous-phase reaction(s), and (e) mass transport of reaction product(s) and possible subsequent evolution into the gas phase. We assumed a fixed ratio of bromine species could be recycled back to the gas phase from the aqueous phase, with the remainder lost to aerosol surfaces (See the "Chemical box modeling" section below for the method to determine the ratio value).

$$\frac{d[X]_{\mathrm{aq}}}{\mathrm{dt}} = k_{\mathrm{mt}} \times [X]_g - \frac{k_{\mathrm{mt}}}{K_H \times R \times T} \times [X]_{\mathrm{aq}} \quad (2)$$

$$\frac{d[X]_g}{\mathrm{dt}} = \frac{k_{\mathrm{mt}} \times \mathrm{LWC}}{K_H \times R \times T} \times [X]_{\mathrm{aq}} \times \mathrm{Ratio} - k_{\mathrm{mt}} \times \mathrm{LWC} \times [X]_g \quad (3)$$

where $[X]_g$ and $[X]_{\mathrm{aq}}$ represent the gas-phase and aqueous-phase concentrations of bromine species. We assumed that the particle phase is predominantly aqueous, given the humid conditions (well above the initial efflorescence relative humidity range summarized in Ma et al. (2021)) and the significant aerosol water content at the three sites (Figure S1 in Supporting Information S1); k_{mt} represents the mass transport coefficient, which was determined based on Equation 4; LWC represents the liquid water content; K_H represents the Henry constant; R represents the molar gas constant; T represents the ambient temperature; and "Ratio" represents the ratio of $[X]_{\mathrm{aq}}$ that was recycled into $[X]_g$. Refer to Text S2 in Supporting Information S1 for the quantum calculation on K_H values.

$$k_{mt} = \left(\frac{r^2}{3D_g} + \frac{4r}{3 < c > \alpha}\right)^{-1} \quad (4)$$

where r denotes the particle radius; D_g denotes the gas-phase diffusion coefficient, which was estimated using Fuller-Schettler-Giddings equation; $<c>$ represents the mean velocity of the gas molecules; and α represents the mass accommodation coefficient. Refer to Table S2 in Supporting Information S1 for the values and references of D_g and α for individual bromine species.

2.3. Multiphase Chemical Box Modeling

We conducted five sets of simulations using the chemical box model powered by Framework for 0-D Atmospheric Modeling (F0AM) (Wolfe et al., 2016). Observational data collected from HT, CVAO, and WD were averaged or interpolated into 5-min resolution over a 24-hr period. Each simulation was initiated at 00:00 local time (LT) and ended at 23:55 LT, with an integration step of 5 min. The bromine species were initialized according to observational data, and then, their formation and chemistry were simulated freely with inputs of relevant species in the following integration. To stabilize the concentrations of unconstrained species, the model was prerun for 1 day to approach a steady state, and results from the second day were extracted for analysis. The details of model scenarios are provided in Table 1 and Table S3 in Supporting Information S1 and are summarized below.

The first set examined the impact of nitrate photodissociation on bromine levels, using identical inputs derived from HT observations (Table S3 in Supporting Information S1) for both MECH_EX and MECH_NO_3^- simulations. The inputs of unmeasured species or parameters were handled as follows: aqueous-phase Br^- concentrations were estimated by assuming the same Cl^- to Br^- ratio in the aerosol phase as that in the seawater (i.e., $[Cl^-]/[Br^-] = 650:1$) (Xia et al., 2022). Based on such assumption, the Br^- concentration was determined to be 0.003 ± 0.00038 mol/L (Figure S1 in Supporting Information S1), under which the inhibitory effect of Cl^- on Br_2 release can be considered negligible (Finlayson-Pitts, 2003); the particle radius was calculated from the measured particle number and size distribution, assuming spherical particles; and LWC and aerosol H^+ concentrations were calculated using ISORROPIA II with forward mode and metastable state assumption (Guo et al., 2015, 2016). The results from ISORROPIA II simulations for NH_3 show good agreement with the observed NH_3 concentrations (Figure S2 in Supporting Information S1). The differences in bromine species concentrations simulated with MECH_EX and MECH_NO_3^- indicate the impact of nitrate photodissociation.

The second set determined the ratio of bromine species lost on aerosol surfaces, using HT-derived inputs as in the first set (Table 1 and Table S3 in Supporting Information S1). These simulations, performed with MECH_PT*X* (where *X* denotes the assumed ratio value of bromines that can be recycled from the aqueous phase to the gas phase, varying from 0 to 1 in 0.05 increments), identified a recycling ratio of 0.80 for MECH_PT, when both the simulated Br_2 and BrCl concentrations agreed well with observations at HT (Figure S3 in Supporting Information S1).

The third set examined the impact of heterogeneous loss of individual bromine species on total reactive bromine (Br_y) levels, using HT-derived inputs as in the first set (Table 1 and Table S3 in Supporting Information S1). These simulations were performed with MECH_PT_*X*, which extends MECH_NO_3^- by incorporating the aerosol surface loss of each bromine species individually (PT_*X* in Figure S4 in Supporting Information S1, with *X* representing the specific bromine species). The differences in Br_y concentrations between MECH_NO_3^- and MECH_PT_*X* simulations indicate the impact of each species' heterogeneous loss.

The fourth set examined the impact of aerosol-related multiphase processes (i.e., nitrate photodissociation and heterogeneous loss on aerosol surfaces) on bromine chemistry across remote marine, semipolluted coastal, and polluted continental regions. Using identical inputs for each site (Table 1 and Table S3 in Supporting Information S1), simulations were performed with MECH_EX and MECH_PT, respectively. The differences in Br_y concentrations and related reaction rates between MECH_EX and MECH_PT simulations indicate the impact of these multiphase processes.

The fifth set examined the impact of reactive bromine species on O_3 in remote marine, semipolluted coastal, and polluted continental regions. Using identical inputs for each site (Table 1 and Table S3 in Supporting

Journal of Geophysical Research: Atmospheres

10.1029/2024JD042040

Table 1
Summary of Model Scenarios and Corresponding Inputs, Mechanisms, and Motivations

Scenario	ID	Input	Mechanism	Motivation
The first set of simulations	Sim_{1-1}	HT input	MECH_EX	Quantify the impact of nitrate photodissociation on bromine levels by comparing the simulated concentrations of bromine species from Sim_{1-1} and Sim_{1-2}
	Sim_{1-2}		MECH_NO_3^-	
The second set of simulations	Sim_{2-1}–Sim_{2-20}	HT input	MECH_PT0–MECH_PT0.95, with a bin precision of 0.05	Determine the ratio of bromine species that were lost on the aerosol surface by comparing the simulated Br_2 and BrCl concentrations from Sim_{2-1}–Sim_{2-20} with observations at HT
The third set of simulations	Sim_{3-1}–Sim_{3-7}	HT input	MECH_PT_*X*, *X* denotes Br_2, BrCl, BrO, $BrNO_2$, $BrNO_3$, HOBr, and HBr, respectively	Examine the impact of the heterogeneous loss of individual bromine species on Br_y levels by comparing the simulated Br_y concentrations from Sim_{3-1}–Sim_{3-7} with those from Sim_{1-2}
The fourth set of simulations	Sim_{4-1}	CVAO input	MECH_EX	Examine the impact of aerosol-related multiphase processes on bromine chemistry by comparing the simulated Br_y concentrations from Sim_{4-1}, Sim_{4-3}, and Sim_{4-5} with those from Sim_{4-2}, Sim_{4-4}, and Sim_{4-6}
	Sim_{4-2}		MECH_PT	
	Sim_{4-3}	HT input	MECH_EX	
	Sim_{4-4}		MECH_PT	
	Sim_{4-5}	WD input	MECH_EX	
	Sim_{4-6}		MECH_PT	
The fifth set of simulations	Sim_{5-1}	CVAO input	MECH_EX without considering bromine chemistry	Examine the impact of reactive bromine species on O_3 by comparing the simulated O_x (=O_3 + NO_2) production and destruction rates from Sim_{5-1}, Sim_{5-4}, and Sim_{5-7} with those from Sim_{5-3} (or Sim_{5-2}), Sim_{5-6} (or Sim_{5-5}), and Sim_{5-9} (or Sim_{5-8})
	Sim_{5-2}		MECH_EX	
	Sim_{5-3}		MECH_PT	
	Sim_{5-4}	HT input	MECH_EX without considering bromine chemistry	
	Sim_{5-5}		MECH_EX	
	Sim_{5-6}		MECH_PT	
	Sim_{5-7}	WD input	MECH_EX without considering bromine chemistry	
	Sim_{5-8}		MECH_EX	
	Sim_{5-9}		MECH_PT	

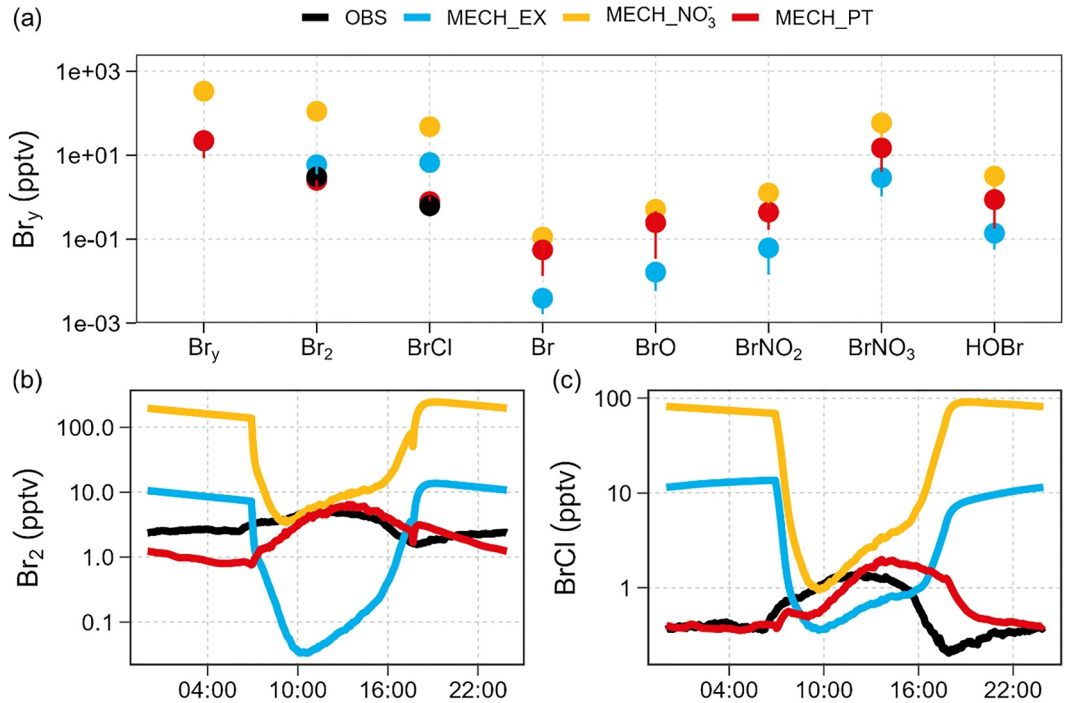

Figure 1. The model-simulated bromine species concentration using different chemical mechanisms and comparisons with observations at a coastal site (Hok Tsui, Hong Kong). The panels were shown in log10 scales. (a) Average concentrations of Br_2, $BrNO_2$, BrCl, Br, BrO, $BrNO_3$, HOBr, and Br_y (=2 × Br_2 + $BrNO_2$ + BrCl + Br + BrO + $BrNO_3$ + HOBr). Error bars indicate half the standard deviation of the mean. (b) Diurnal profiles of Br_2 concentrations. (c) Diurnal profiles of BrCl concentrations. OBS: observations. MECH_EX: existing mechanisms; MECH_NO_3^-: MECH_EX + nitrate photodissociation; MECH_PT: MECH_NO_3^- + heterogeneous loss on the aerosol surface of Br_2, BrCl, BrO, $BrNO_2$, $BrNO_3$, HOBr, and HBr.

Information S1), simulations were performed without bromine chemistry and with MECH_EX and MECH_PT, respectively. Like bromine species, the concentration of O_3 was initialized according to observational data, and then, its formation and chemistry were simulated freely with inputs of relevant species in the following integration. Instead of a direct 1-day prerun, oxygenated VOC concentrations were initialized according to prerun results. The differences in the net rates of O_x (=O_3 + NO_2) production calculated with and without bromine chemistry indicate the impact of reactive bromine species on O_3. We focused on the net rate of O_x production to eliminate the effect of NO titration on O_3 (see Text S3 in Supporting Information S1 for the calculation of the net rates of O_x production).

3. Results and Discussion

3.1. Aerosol-Related Multiphase Processes and Impact on Bromine Species

Figure 1 compares bromine simulations and observations at the HT site. Using the MECH_EX mechanism, the simulated Br_2 and BrCl concentrations peaked in the nighttime, in contrast to the observed daytime peaks. The average simulated concentrations for Br_2 and BrCl were 5.9 ± 5.2 pptv and 6.7 ± 5.3 pptv, respectively, modestly higher than observations (3.0 ± 1.0 pptv for Br_2 and 0.62 ± 0.38 pptv for BrCl). These discrepancies highlighted the inadequacy of polar-derived mechanisms in capturing the diurnal patterns of bromine species in extrapolar regions.

We incorporated nitrate photodissociation, a bromine activation pathway (Abbatt et al., 2010; Dalton et al., 2023; George & Anastasio, 2007) parameterized based on the HT studies (Xia et al., 2022), into the model, that is, the MECH_NO_3^- mechanism. This adaptation allowed the model to reproduce the significant daytime bromine concentrations observed (Figure 1). However, it also led to an overestimation of nighttime bromine levels (simulations: 110 ± 92 pptv for Br_2 and 48 ± 37 pptv for BrCl; observations: 3.0 ± 1.0 pptv for Br_2 and 0.62 ± 0.38 pptv for BrCl), suggesting the presence of unaccounted-for bromine sinks.

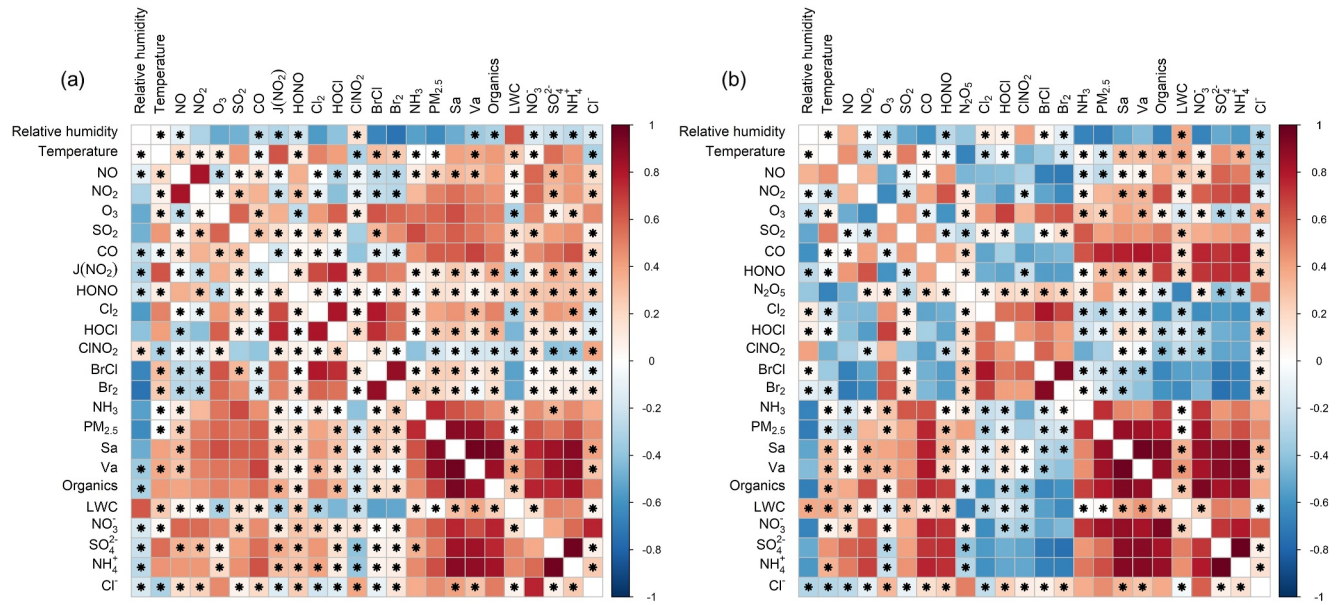

Figure 2. Correlations (*r*-value) between reactive halogen species and other species or parameters at Hok Tsui. (a) Correlations during the daytime, specifically from 6:00 to 18:00 LT. (b) Correlations during the nighttime, specifically from 19:00 to 5:00 LT. Results with a low significance level ($p > 0.05$) were marked with black markers.

We further examined correlations between reactive bromine species and other species or parameters, leading to the correlation matrix of Figure 2. Here, daytime and nighttime averages were used to minimize diurnal variation effects. A positive correlation was found with $J(NO_2)$ in the daytime (related to Br_2 production from nitrate photodissociation) and with O_3 in both the daytime and nighttime (attributed to HOBr production from the heterogeneous reactions of O_3). In contrast, a significant negative correlation was observed with aerosols during the night. Negative correlations with aerosol liquid water content and relative humidity further pointed to the role of heterogeneous uptake on aerosol surfaces in bromine loss, with the rate influenced by aerosol liquid water content. Within major aerosol compositions, bromine species were negatively correlated with sulfate (r: −0.74), ammonium (r: −0.69), and organics (r: −0.60), and to a lesser extent with nitrate (r: −0.45) (Figure S5 in Supporting Information S1). This is because nitrate aerosols can influence both bromine activation and bromine loss.

To implement the heterogeneous loss of bromine species on aerosol surfaces, we integrated phase transfer processes (Ervens et al., 2003; Hoffmann et al., 2019), involving both gas-to-aqueous and aqueous-to-gas mass transport, into the MECH_NO_3^- mechanism (i.e., the MECH_PT mechanism). Using the MECH_PT mechanism, the average simulated concentrations for Br_2 and BrCl were 2.5 ± 1.7 pptv and 0.78 ± 0.52 pptv, respectively, with both species peaking in the daytime (Figure 1). Additionally, we noted a slight delay in the simulated daytime BrCl peak, as well as lower nighttime BrCl concentrations than observations. These discrepancies could be attributed to unaccounted-for reactions among bromine species that may not be fully represented in the current model setup. The incorporation of nitrate photodissociation and heterogeneous loss on the aerosol surface into the polar-derived mechanisms reproduced the observed bromine concentrations and patterns at HT, highlighting the significance of aerosol-related multiphase processes in bromine chemistry. On a species level, the heterogeneous loss of $BrNO_3$ had the largest effect on Br_y concentrations (−88%), followed by Br_2 (−59%), HOBr (−18%), and BrCl (−18%) (Figure S4 in Supporting Information S1). This is due to their high abundance and high probability of colliding with the aerosol surface to enter the particle phase (indicated by larger mass accommodation coefficient values of $BrNO_3$, HOBr, and BrCl) or high solubility in the aqueous phase (indicated by larger Henry constant values of HOBr and Br_2) (Table S2 in Supporting Information S1).

Simulations at Cape Verde and Wangdu sites with both MECH_EX and MECH_PT mechanisms further validated the impact of aerosol-related multiphase processes across different extrapolar marine and continental environments. The MECH_PT mechanism improved bromine simulations, especially in capturing the daytime bromine peaks at WD and the significant loss of BrCl on aerosol surfaces at CVAO (Figures S6a and S6b in Supporting

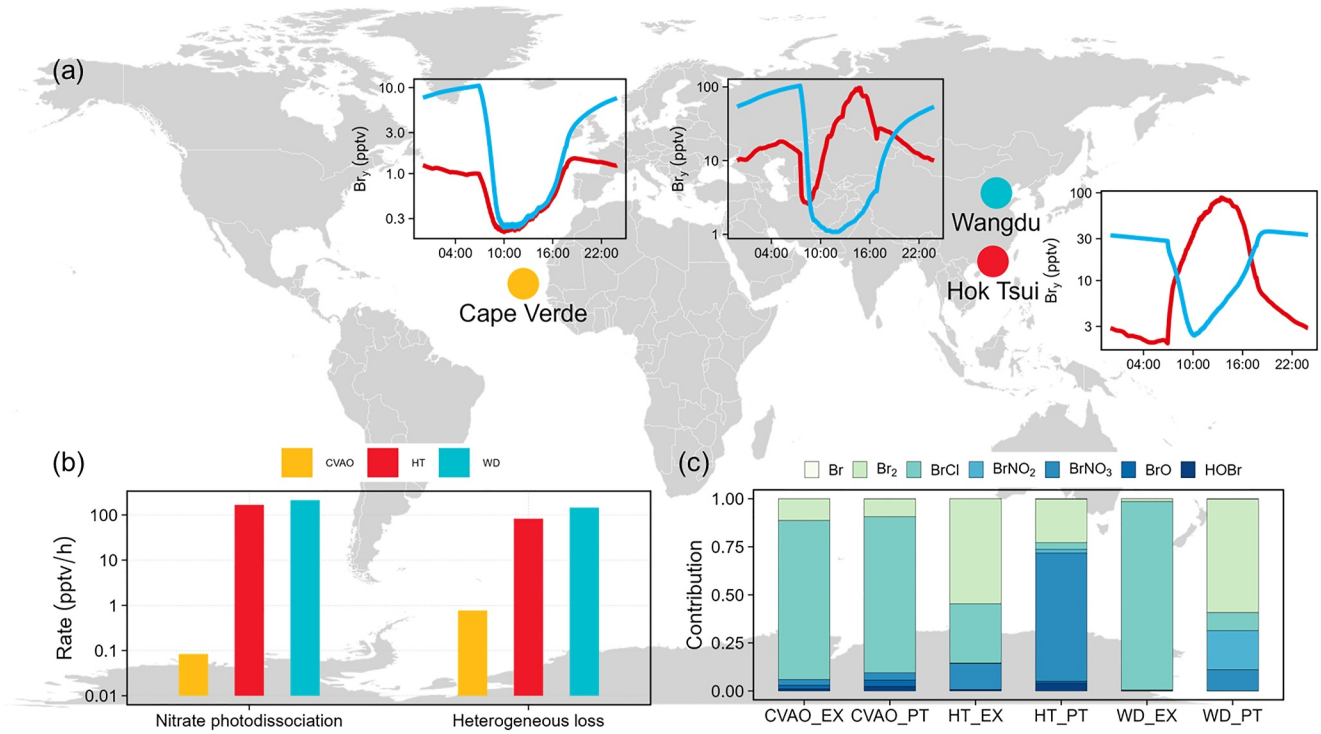

Figure 3. (a) Comparison of model-simulated Br_y concentrations with MECH_EX and MECH_PT. (b) The model-calculated rates (shown in log10 scales) of Br_2 production from nitrate photodissociation and Br_y loss on the aerosol surface with MECH_PT. (c) The model-simulated Br_y chemical speciation with MECH_EX and MECH_PT, respectively.

Information S1). Previous modeling studies did not consider aerosol-related multiphase processes and consequently overestimated BrCl and total bromine levels in the MBL (Long et al., 2014; Sommariva & von Glasow, 2012). Overall, the MECH_PT mechanism offers a reasonable explanation for bromine observations across diverse extrapolar environments.

3.2. Key Factors Driving the Bromine Recycling in Extrapolar Regions

We further examined the impact of multiphase processes on bromine recycling in extrapolar regions. A key finding is the regulation of aerosol-related multiphase processes on the diurnal variations of bromine species, primarily through modulation of the partitioning between the gas and aqueous phases. With the MECH_EX mechanism, Br_y concentrations peaked during the nighttime at all three extrapolar sites. However, using the MECH_PT mechanism, we found increased daytime Br_y concentrations at both HT and WD, in contrast to CVAO, where nighttime peaks persisted (Figure 3a).

At the HT and WD sites, characterized by either high aerosol acidity and/or aerosol load (Figure S1 in Supporting Information S1), the process of nitrate photodissociation is a crucial mechanism for the daytime recycling of bromide back into the gas phase, with average rates of 170 ± 250 pptv/hr (HT) and 210 ± 400 pptv/hr (WD) (i.e., bromine molecule production rate from nitrate photodissociation), respectively. Concurrently, the high aerosol liquid water content at these sites facilitated the rapid loss of gaseous bromine species to aerosol surfaces, at rates of 82 ± 110 pptv/hr (HT) and 150 ± 150 pptv/hr (WD), respectively (Figure 3b). The net effect of these processes was a pronounced increase in Br_y levels during the daytime, attributed mainly to the dominance of nitrate photodissociation over heterogeneous loss. In comparison, the CVAO's relatively low aerosol abundance and weak acidity resulted in negligible rates of aerosol-related multiphase processes (0.084 ± 0.11 pptv/hr for nitrate photodissociation; 0.77 ± 0.31 pptv/hr for heterogeneous loss). Consequently, nighttime Br_y peaks persisted at the CVAO site.

The chemical speciation of Br_y was also affected by aerosol-related processes (Figure 3c). Using the MECH_EX mechanism, BrCl was the predominant species at CVAO (83%) and WD (98%), while Br_2 predominated at HT

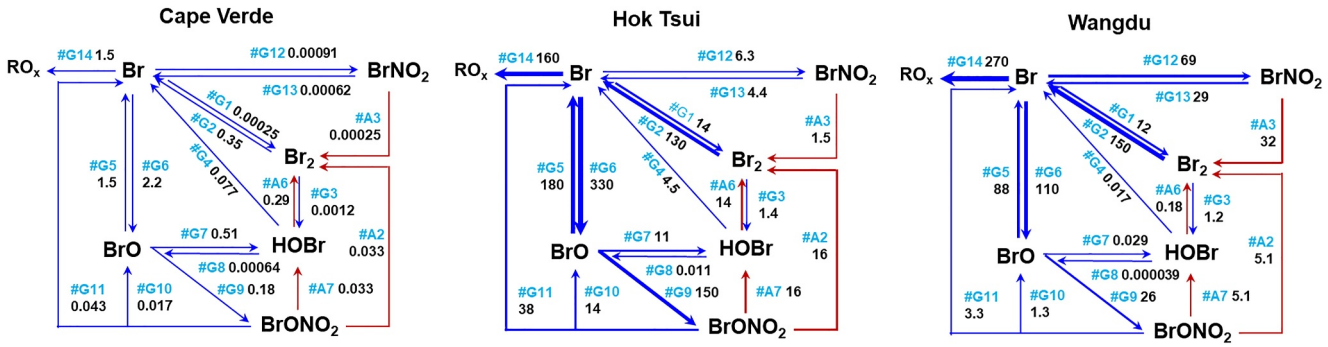

Figure 4. The model-simulated rate of the chemical sources and sinks of gaseous bromine species (unit: pptv/h) at Cape Verde, Hok Tsui, and Wangdu using MECH_PT. The blue and red lines denote gaseous reactions and uptake reactions, respectively. Refer to Table S4 in Supporting Information S1 for an extensive explanation of the pathways.

(55%). Using the MECH_PT mechanism, there was a significant reduction in BrCl's contribution across the three sites (from 31%–98% to 4%–81%), due to its rapid aerosol surface loss relative to other bromine species. In comparison, species like BrO, HOBr, $BrNO_2$, and $BrNO_3$ saw increased contributions at varying extents. For BrO and $BrNO_2$, the increased contributions (from 0%–2% to 0%–3% for BrO; from 0%–0% to 0%–20% for $BrNO_2$) were due to their slower aerosol surface loss rates. For HOBr and $BrNO_3$, their production from accumulated BrO offset their aerosol surface loss (Figure 4), leading to their increased contributions (from 0%–1% to 0%–4% for HOBr; from 0%–14% to 4%–67% for $BrNO_3$). The impact of aerosol-related processes on Br_2 was complex, with Br_2's contribution decreasing at HT (from 55% to 23%) but increasing at WD (from 1% to 59%) using the MECH_PT mechanism. This difference is attributed to the faster conversion of Br_2 from $BrNO_2$ uptake at WD than $BrNO_3$ uptake at HT.

Additionally, the Br_y chemical speciation was affected by the abundance of oxidants and NO_x, and this pattern was consistent for simulations with both MECH_EX and MECH_PT (Figure 4 and Figure S7 in Supporting Information S1). For further analysis, we focused on the results from MECH_PT. Among the three extrapolar sites, WD represents a high-NO_x (mean ± sd: 83 ± 35 ppbv for NO_x) and low-oxidant (mean ± sd: 8.3 ± 5.2 ppbv for O_3) condition, HT represents a moderate-NO_x (mean ± sd: 3.5 ± 0.67 ppbv for NO_x) and high-oxidant (mean ± sd: 50 ± 9.8 ppbv for O_3) condition, and CVAO represents a low-NO_x (mean ± sd: 0.023 ± 0.0079 ppbv for NO_x) and moderate-oxidant (mean ± sd: 29 ± 0.99 ppbv for O_3) condition (Figure S1 in Supporting Information S1). The oxidants and NO_x levels are important for the recycling of reactive bromine species like Br and BrO radicals to less reactive species like $BrNO_x$ and HOBr. For instance, under moderate-to-high-oxidant and low-to-moderate-NO_x conditions, Br radical predominantly reacted with O_3/NO_3 radical/ClO_2 radical to form BrO radical (#G6-#G5 in Figure 4; CVAO: 0.69 ± 0.79 pptv/hr; HT: 150 ± 230 pptv/hr), while at the high-NO_x and low-oxidant WD site, Br radical favored forming $BrNO_2$ (#G12-#G13 in Figure 4; 40 ± 72 pptv/hr). This resulted in a higher $BrNO_2$ proportion at WD (20%) than HT (2%) and CVAO (0%). Additionally, the fate of BrO radical varied with NO_x levels. Under moderate-NO_x concentration levels at the HT site, BrO radical was rapidly converted to $BrNO_3$ (#G9-#G10 in Figure 4; 130 ± 210 pptv/hr), leading to its significant contribution (67%) to Br_y, whereas at low-NO_x condition at the CVAO site, BrO radical predominantly formed HOBr (#G7–#G8 in Figure 4; 0.51 ± 0.59 pptv/hr).

3.3. Larger Effects of Bromine Species on Ozone in Polluted Regions Than Previously Thought

As shown in the proceeding section, the aerosol-related multiphase process strongly affected bromine chemistry. Here, we assessed the impacts of bromine species on O_3 by comparing the net rates of O_x production calculated without considering bromine chemistry and with MECH_PT (as outlined in the fifth set in Chemical box modeling). At CVAO, bromine species slightly reduced the net O_x production rates by −0.0011 ppbv/hr (−2%), whereas at HT and WD, bromine species increased the net O_x production rates by 0.039 ppbv/hr (1%) and 0.63 ppbv/hr (23%), respectively (Figure 5 and Figure S8 in Supporting Information S1). These results are consistent with previous studies (Peng et al., 2020; Read et al., 2008; Thompson et al., 2017; Wang et al., 2019; Xia et al., 2022), indicating that Br radical consumes O_3 in polar and pristine MBL environments with low VOC levels (e.g., mean ± sd: 2.0 ± 0.17 ppbv for C_2-C_{10} species at CVAO) but enhances O_3 levels in semipolluted and

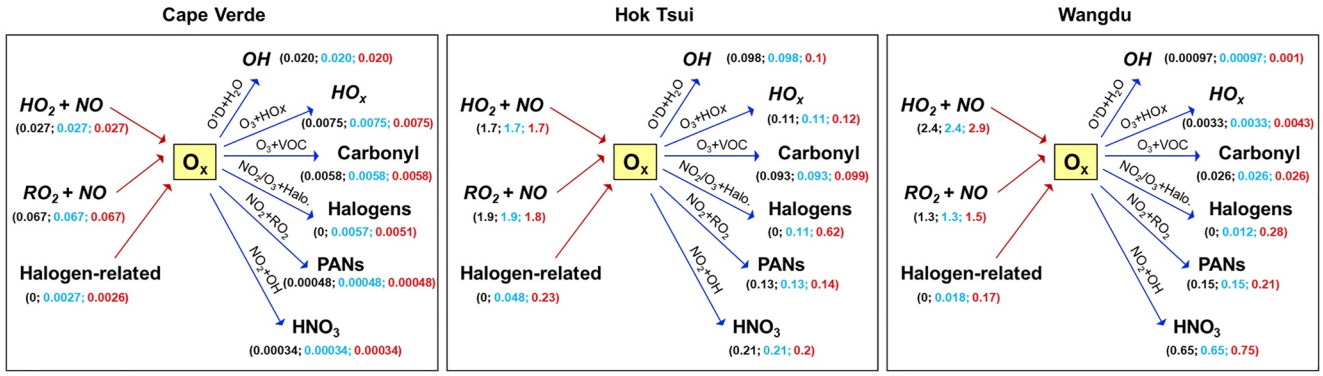

Figure 5. The model-simulated rate of O_x chemical production and destruction (unit: ppbv/h) using different chemical mechanisms. The black, blue, and red values indicate average rates without considering bromine chemistry, using MECH_EX and MECH_PT, respectively. Refer to Text S3 in Supporting Information S1 for the definition of the "halogen-related" factor.

polluted regions with modest-to-high VOC levels (e.g., mean ± sd: 7.7 ± 0.47 ppbv for C_2–C_{10} species at HT and 63 ± 22 ppbv for C_2–C_{10} species at WD). The incorporation of bromine chemistry can accelerate the rates of both O_x production and O_x destruction, and the impact on O_x production outweighed that on O_x destruction at HT and WD, leading to an overall increase in net O_x production, in contrast to the bromine effect at CVAO (Figure 5). Notably, despite comparable daytime Br_y concentrations at HT and WD (Figure 3), bromine species exerted a larger influence on O_x-related rates at WD. This discrepancy can be attributed to the more pronounced impact of bromine species on RO_x radical (=OH + HO_2 + RO_2) cycling at WD (270 pptv/hr) than HT (160 pptv/hr) (Figure 4).

We further compared the impact of bromine species on net O_x production rates using MECH_EX and MECH_PT mechanisms (Figure 5 and Figure S8 in Supporting Information S1). The incorporation of aerosol-related processes resulted in a considerable change in the effect of bromine species on O_x production. Specifically, the transition from MECH_EX to MECH_PT shifted the impact of bromine species from negative (−0.0092 ppbv/hr) to positive (0.039 ppbv/hr) on net O_x production rates at HT and amplified the positive impact at WD (by 0.62 ppbv/hr), with minimal changes found at CVAO. These results underscore the potential underestimation of reactive bromine species' role in photochemical ozone production within semipolluted (e.g., mean ± sd: 18 ± 7.5 μg/m^3 for $PM_{2.5}$ at HT) and polluted (e.g., mean ± sd: 140 ± 36 μg/m^3 for $PM_{2.5}$ at WD) regions when aerosol-related multiphase processes are overlooked.

4. Uncertainties, Implications, and Outlook

This study highlights the dual effect of aerosols on bromine recycling and the significant impact of the aerosol-related multiphase process on bromine chemistry outside the polar regions under both marine and continental conditions. This dual effect included the efficient recycling of bromide into the gas phase in regions characterized by strong aerosol acidity or abundant aerosols and the significant aerosol surface loss of bromine species at high liquid water content. Our study contributes to a deeper understanding of the lower-than-expected low levels of reactive bromine species in the MBL atmosphere and elucidates the mechanisms behind pollution-related bromine recycling in semipolluted and polluted regions. Additionally, similar aerosol-driven multiphase processes are suggested to occur within chlorine chemistry, as inferred from correlation analyses between reactive chlorine species and other species or parameters (Figure 2). Overlooking these processes would hinder the accurate assessment of the impact of reactive halogens on climate and air quality.

Despite improvement in our model's representation of bromine chemistry, considerable discrepancies between observed and simulated results remain (Figure S6 in Supporting Information S1). For example, the model underestimates bromine concentrations at WD, likely due to unaccounted-for direct emissions from coal burning (Peng et al., 2020). Furthermore, the diurnal patterns of bromine species, particularly BrCl, were not well captured at WD, potentially because the model applied the same recycling ratio of bromine species from the aqueous to the gas phase as at HT, which should vary depending on site-specific conditions. The model simulation also suggests high levels of $BrNO_3$ in semipolluted coastal and polluted continental regions, which were not detected by the

CIMS at HT and WD. This discrepancy may be attributed to an underestimation of heterogeneous loss of $BrNO_3$ due to a uniform recycling ratio from the aqueous to the gas phase across all bromine species.

To address these uncertainties, future efforts should focus on establishing a more elaborate multiphase halogen chemistry module, with specific attention to (a) acquiring kinetic data for the phase transfer process (or uptake coefficients) of key halogen species, particularly for those with limited experimental values, such as $BrNO_2$ and BrO (Text S2 in Supporting Information S1) (Sander, 2015) and (b) developing a comprehensive aqueous-phase halogen chemistry mechanism, or at least determining accurate loss ratios of major reactive halogen species on aerosol surfaces. Furthermore, measurements of bromine species remain limited due to their low concentration levels and the high precision required for instrumentation. More extensive field measurements are necessary to validate model-based predictions and to enhance our understanding of bromine recycling.

Conflict of Interest

The authors declare no conflicts of interest relevant to this study.

Data Availability Statement

The code of the MCM box model can be accessed from the Zenodo open data repository (Wolfe & Haskins, 2023). The code of CAPRAM is available at https://capram.tropos.de/.

Acknowledgments
We thank the Master Chemical Mechanism and Chemical Aqueous-Phase RAdical Mechanism development groups for the provision of the mechanisms. We also thank Dr. Glenn Wolfe for the provision of the F0AM platform. This work was sponsored by the National Natural Science Foundation of China, China (42293322), the Hong Kong Research Grants Council, China (15207421 and T24-504/17-N), and the Hong Kong Polytechnic University, China (P0042606).

References

Abbatt, J., Oldridge, N., Symington, A., Chukalovskiy, V., McWhinney, R., Sjostedt, S., & Cox, R. (2010). Release of gas-phase halogens by photolytic generation of OH in frozen halide−nitrate solutions: An active halogen formation mechanism. *The Journal of Physical Chemistry A*, *114*(23), 6527–6533. https://doi.org/10.1021/jp102072t

Abbatt, J., Thomas, J., Abrahamsson, K., Boxe, C., Granfors, A., Jones, A., et al. (2012). Halogen activation via interactions with environmental ice and snow in the polar lower troposphere and other regions. *Atmospheric Chemistry and Physics*, *12*(14), 6237–6271. https://doi.org/10.5194/acp-12-6237-2012

Ammann, M., Cox, R. A., Crowley, J., Jenkin, M., Mellouki, A., Rossi, M., et al. (2013). Evaluated kinetic and photochemical data for atmospheric chemistry: Volume VI – Heterogeneous reactions with liquid substrates. *Atmospheric Chemistry and Physics*, *13*(16), 8045–8228. https://doi.org/10.5194/acp-13-8045-2013

Barrie, L., Bottenheim, J., Schnell, R., Crutzen, P., & Rasmussen, R. (1988). Ozone destruction and photochemical reactions at polar sunrise in the lower Arctic atmosphere. *Nature*, *334*(6178), 138–141. https://doi.org/10.1038/334138a0

Bottenheim, J., Gallant, A., & Brice, K. (1986). Measurements of NO_Y species and O_3 at 82°N latitude. *Geophysical Research Letters*, *13*(2), 113–116. https://doi.org/10.1029/GL013i002p00113

Dalton, E., Hoffmann, E., Schaefer, T., Tilgner, A., Herrmann, H., & Raff, J. (2023). Daytime atmospheric halogen cycling through aqueous-phase oxygen atom chemistry. *Journal of the American Chemical Society*, *145*(29), 15652–15657. https://doi.org/10.1021/jacs.3c03112

Ervens, B., George, C., Williams, J., Buxton, G., Salmon, G., Bydder, M., et al. (2003). CAPRAM 2.4 (MODAC mechanism): An extended and condensed tropospheric aqueous phase mechanism and its application. *Journal of Geophysical Research*, *108*(D14), 4426. https://doi.org/10.1029/2002JD002202

Finlayson-Pitts, B. J. (2003). The tropospheric chemistry of sea salt: A molecular-level view of the chemistry of NaCl and NaBr. *Chemical Reviews*, *103*(12), 4801–4822. https://doi.org/10.1021/cr020653t

George, I., & Anastasio, C. (2007). Release of gaseous bromine from the photolysis of nitrate and hydrogen peroxide in simulated sea-salt solutions. *Atmospheric Environment*, *41*(3), 543–553. https://doi.org/10.1016/j.atmosenv.2006.08.022

Guo, H., Sullivan, A., Campuzano-Jost, P., Schroder, J., Lopez-Hilfiker, F., Dibb, J., et al. (2016). Fine particle pH and the partitioning of nitric acid during winter in the northeastern United States. *Journal of Geophysical Research: Atmospheres*, *121*(17), 10355–310376. https://doi.org/10.1002/2016JD025311

Guo, H., Xu, L., Bougiatioti, A., Cerully, K., Capps, S., Hite, J., Jr., et al. (2015). Fine-particle water and pH in the southeastern United States. *Atmospheric Chemistry and Physics*, *15*(9), 5211–5228. https://doi.org/10.5194/acp-15-5211-2015

Hoffmann, E., Tilgner, A., Vogelsberg, U., Wolke, R., & Herrmann, H. (2019). Near-Explicit multiphase modeling of halogen chemistry in a mixed urban and maritime coastal area. *ACS Earth and Space Chemistry*, *3*(11), 2452–2471. https://doi.org/10.1021/acsearthspacechem.9b00184

Jenkin, M., Saunders, S., Wagner, V., & Pilling, M. (2003). Protocol for the development of the Master Chemical Mechanism, MCM v3 (Part B): Tropospheric degradation of aromatic volatile organic compounds. *Atmospheric Chemistry and Physics*, *3*(1), 181–193. https://doi.org/10.5194/acp-3-181-2003

Li, Q., Fernandez, R., Hossaini, R., Iglesias-Suarez, F., Cuevas, C., Apel, E., et al. (2022). Reactive halogens increase the global methane lifetime and radiative forcing in the 21st century. *Nature Communications*, *13*(1), 2768. https://doi.org/10.1038/s41467-022-30456-8

Li, Q., Fu, X., Peng, X., Wang, W., Badia, A., Fernandez, R., et al. (2021). Halogens enhance haze pollution in China. *Environmental Science & Technology*, *55*(20), 13625–13637. https://doi.org/10.1021/acs.est.1c01949

Liu, T., & Abbatt, J. (2020). An experimental assessment of the importance of S(IV) oxidation by hypohalous acids in the marine atmosphere. *Geophysical Research Letters*, *47*(4), e2019GL086465. https://doi.org/10.1029/2019GL086465

Long, M., Keene, W., Easter, R., Sander, R., Liu, X., Kerkweg, A., & Erickson, D. (2014). Sensitivity of tropospheric chemical composition to halogen-radical chemistry using a fully coupled size-resolved multiphase chemistry–global climate system: Halogen distributions, aerosol composition, and sensitivity of climate-relevant gases. *Atmospheric Chemistry and Physics*, *14*(7), 3397–3425. https://doi.org/10.5194/acp-14-3397-2014

Ma, S., Pang, S., Li, J., & Zhang, Y. (2021). A review of efflorescence kinetics studies on atmospherically relevant particles. *Chemosphere*, *277*, 130320–130338. https://doi.org/10.1016/j.chemosphere.2021.130320

McElroy, C., McLinden, C., & McConnell, J. (1999). Evidence for bromine monoxide in the free troposphere during the Arctic polar sunrise. *Nature*, *397*(6717), 338–341. https://doi.org/10.1038/16904

Oltmans, S., & Komhyr, W. (1986). Surface ozone distributions and variations from 1973–1984: Measurements at the NOAA geophysical monitoring for climatic change baseline observatories. *Journal of Geophysical Research*, *91*(D4), 5229–5236. https://doi.org/10.1029/JD091iD04p05229

Parrella, J., Jacob, D., Liang, Q., Zhang, Y., Mickley, L., Miller, B., et al. (2012). Tropospheric bromine chemistry: Implications for present and pre-industrial ozone and mercury. *Atmospheric Chemistry and Physics*, *12*(15), 6723–6740. https://doi.org/10.5194/acp-12-6723-2012

Peng, X., Wang, W., Xia, M., Chen, H., Ravishankara, A., Li, Q., et al. (2020). An unexpected large continental source of reactive bromine and chlorine with significant impact on wintertime air quality. *National Science Review*, *8*(7), nwaa304. https://doi.org/10.1093/nsr/nwaa304

Platt, U., & Hönninger, G. (2003). The role of halogen species in the troposphere. *Chemosphere*, *52*(2), 325–338. https://doi.org/10.1016/S0045-6535(03)00216-9

Read, K., Mahajan, A., Carpenter, L., Evans, M., Faria, B., Heard, D., et al. (2008). Extensive halogen-mediated ozone destruction over the tropical Atlantic Ocean. *Nature*, *453*(7199), 1232–1235. https://doi.org/10.1038/nature07035

Saiz-Lopez, A., Fernandez, R., Li, Q., Cuevas, C., Fu, X., Kinnison, D., et al. (2023). Natural short-lived halogens exert an indirect cooling effect on climate. *Nature*, *618*(7967), 967–973. https://doi.org/10.1038/s41586-023-06119-z

Saiz-Lopez, A., & von Glasow, R. (2012). Reactive halogen chemistry in the troposphere. *Chemical Society Reviews*, *41*(19), 6448–6472. https://doi.org/10.1039/C2CS35208G

Sander, R. (2015). Compilation of Henry's law constants (version 4.0) for water as solvent. *Atmospheric Chemistry and Physics*, *15*(8), 4399–4981. https://doi.org/10.5194/acp-15-4399-2015

Saunders, S., Jenkin, M., Derwent, R., & Pilling, M. (2003). Protocol for the development of the Master Chemical Mechanism, MCM v3 (Part A): Tropospheric degradation of non-aromatic volatile organic compounds. *Atmospheric Chemistry and Physics*, *3*(1), 161–180. https://doi.org/10.5194/acp-3-161-2003

Simpson, W., Brown, S., Saiz-Lopez, A., Thornton, J., & von Glasow, R. (2015). Tropospheric halogen chemistry: Sources, cycling, and impacts. *Chemical Reviews*, *115*(10), 4035–4062. https://doi.org/10.1021/cr5006638

Simpson, W., von Glasow, R., Riedel, K., Anderson, P., Ariya, P., Bottenheim, J., et al. (2007). Halogens and their role in polar boundary-layer ozone depletion. *Atmospheric Chemistry and Physics*, *7*(16), 4375–4418. https://doi.org/10.5194/acp-7-4375-2007

Sommariva, R., & von Glasow, R. (2012). Multiphase halogen chemistry in the tropical Atlantic Ocean. *Environmental Science & Technology*, *46*(19), 10429–10437. https://doi.org/10.1021/es300209f

Thompson, C., Shepson, P., Liao, J., Huey, L., Cantrell, C., Flocke, F., & Orlando, J. (2017). Bromine atom production and chain propagation during springtime Arctic ozone depletion events in Barrow, Alaska. *Atmospheric Chemistry and Physics*, *17*(5), 3401–3421. https://doi.org/10.5194/acp-17-3401-2017

Wang, S., McNamara, S., Moore, C., Obrist, D., Steffen, A., Shepson, P., et al. (2019). Direct detection of atmospheric atomic bromine leading to mercury and ozone depletion. *Proceedings of the National Academy of Sciences of the United States of America*, *116*(29), 14479–14484. https://doi.org/10.1073/pnas.1900613116

Wennberg, P. (1999). Bromine explosion. *Nature*, *397*(6717), 299–301. https://doi.org/10.1038/16805

Wolfe, G., & Haskins, J. (2023). AirChem/F0AM: V4.3 (v4.3) [Software]. *Zenodo*. https://doi.org/10.5281/zenodo.8305950

Wolfe, G., Marvin, M., Roberts, S., Travis, K., & Liao, J. (2016). The Framework for 0-D Atmospheric Modeling (F0AM) v3.1. *Geoscientific Model Development*, *9*(9), 3309–3319. https://doi.org/10.5194/gmd-9-3309-2016

Xia, M., Wang, T., Wang, Z., Chen, Y., Peng, X., Huo, Y., et al. (2022). Pollution-Derived Br_2 boosts oxidation power of the coastal atmosphere. *Environmental Science & Technology*, *56*(17), 12055–12065. https://doi.org/10.1021/acs.est.2c02434

References From the Supporting Information

Carpenter, L., Fleming, Z., Read, K., Lee, J., Moller, S., Hopkins, J., et al. (2010). Seasonal characteristics of tropical marine boundary layer air measured at the Cape Verde Atmospheric Observatory. *Journal of Atmospheric Chemistry*, *67*(2), 87–140. https://doi.org/10.1007/s10874-011-9206-1

Lawler, M., Finley, B., Keene, W., Pszenny, A., Read, K., von Glasow, R., & Saltzman, E. S. (2009). Pollution-enhanced reactive chlorine chemistry in the eastern tropical Atlantic boundary layer. *Geophysical Research Letters*, *36*(8), L08810. https://doi.org/10.1029/2008GL036666

Lawler, M., Sander, R., Carpenter, L., Lee, J., von Glasow, R., Sommariva, R., & Saltzman, E. S. (2011). HOCl and Cl_2 observations in marine air. *Atmospheric Chemistry and Physics*, *11*(15), 7617–7628. https://doi.org/10.5194/acp-11-7617-2011

Marenich, A., Cramer, C., & Truhlar, D. (2009). Universal solvation model based on solute electron density and on a continuum model of the solvent defined by the bulk dielectric constant and atomic surface tensions. *The Journal of Physical Chemistry B*, *113*(18), 6378–6396. https://doi.org/10.1021/jp810292n

Müller, K., Lehmann, S., Van, D., Gnauk, T., Niedermeier, N., Wiedensohler, A., & Herrmann, H. (2010). Particle characterization at the Cape Verde atmospheric observatory during the 2007 RHaMBLe intensive. *Atmospheric Chemistry and Physics*, *10*(6), 2709–2721. https://doi.org/10.5194/acp-10-2709-2010